AD-A182 422 INVESTIGATION OF SHEATH PHENOMENA IN ELECTRONEGATIVE GLOW DISCHARGES(U) AIR COMMAND AND STAFF COLL MAXWELL AFB AL G L DUKE APR 87 ACSC-87-0730 1/1

UNCLASSIFIED F/G 20/3 NL

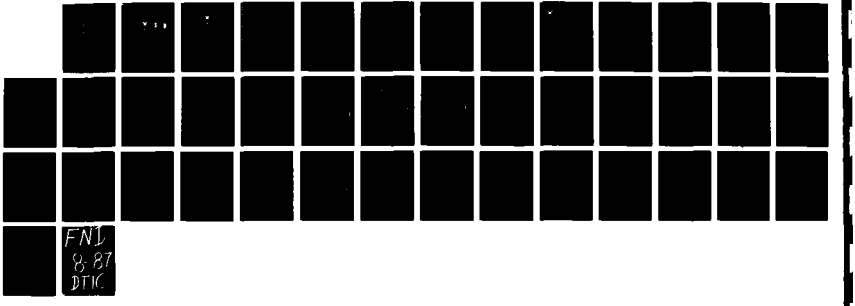

FNL
8-87
DTIC

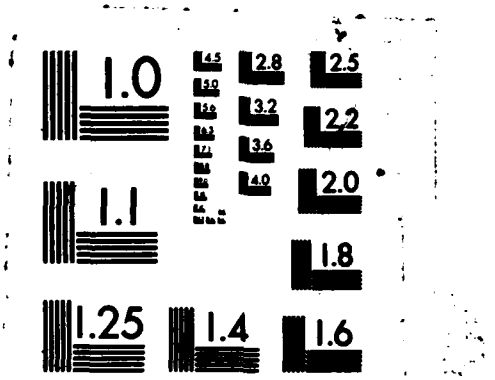

(2)

AIR COMMAND AND STAFF COLLEGE

STUDENT REPORT

INVESTIGATION OF SHEATH PHENOMENA
IN ELECTRONEGATIVE GLOW DISCHARGES

MAJOR GARY L. DUKE, PH.D. 87-0730

"insights into tomorrow"

REPORT NUMBER 87-0730

TITLE INVESTIGATION OF SHEATH PHENOMENA IN ELECTRONEGATIVE GLOW DISCHARGES

AUTHOR(S) MAJOR GARY L. DUKE, PhD, USAF

FACULTY ADVISOR MAJOR DOUGLAS D. DEABLER, ACSC/DO

SPONSOR DR. ALAN GARSCADDEN, AFWAL/POOC-3
Wright-Patterson AFB, OH 45433

Submitted to the faculty in partial fulfillment of requirements for graduation.

AIR COMMAND AND STAFF COLLEGE
AIR UNIVERSITY
MAXWELL AFB, AL 36112

UNCLASSIFIED
SECURITY CLASSIFICATION OF THIS PAGE

A182 422

REPORT DOCUMENTATION PAGE

1a. REPORT SECURITY CLASSIFICATION UNCLASSIFIED	1b. RESTRICTIVE MARKINGS
2a. SECURITY CLASSIFICATION AUTHORITY	3. DISTRIBUTION/AVAILABILITY OF REPORT STATEMENT "A" Approved for public release; Distribution is unlimited.
2b. DECLASSIFICATION/DOWNGRADING SCHEDULE	
4. PERFORMING ORGANIZATION REPORT NUMBER(S) 87-0730	5. MONITORING ORGANIZATION REPORT NUMBER(S)
6a. NAME OF PERFORMING ORGANIZATION ACSC/EDCC 6b. OFFICE SYMBOL (If applicable)	7a. NAME OF MONITORING ORGANIZATION
6c. ADDRESS (City, State and ZIP Code) Maxwell AFB, AL 36112-5542	7b. ADDRESS (City, State and ZIP Code)
8a. NAME OF FUNDING/SPONSORING ORGANIZATION 8b. OFFICE SYMBOL (If applicable)	9. PROCUREMENT INSTRUMENT IDENTIFICATION NUMBER
8c. ADDRESS (City, State and ZIP Code)	10. SOURCE OF FUNDING NOS. PROGRAM ELEMENT NO. / PROJECT NO. / TASK NO. / WORK UNIT NO.
11. TITLE (Include Security Classification) INVESTIGATION OF (cont'd # 16)	
12. PERSONAL AUTHOR(S) Duke, Gary L. Major, USAF	
13a. TYPE OF REPORT 13b. TIME COVERED FROM _____ TO _____	14. DATE OF REPORT (Yr., Mo., Day) 1987 April 15. PAGE COUNT
16. SUPPLEMENTARY NOTATION (11 cont'd) SHEATH PHENOMENA IN ELECTRONEGATIVE GLOW DISCHARGES	
17. COSATI CODES FIELD / GROUP / SUB. GR.	18. SUBJECT TERMS (Continue on reverse if necessary and identify by block number)

19. ABSTRACT (Continue on reverse if necessary and identify by block number)

Investigates sheath phenomena in electronegative glow discharges. Calculations have been performed for He/HCl, Ar/HCl, and Xe/HCl mixtures to model the cathode fall region of a gas discharge. The electric field, Townsend ionization and attachment coefficients, as well as positive ion, negative ion, and electron densities were calculated as a function of distance. Attachment was found to increase the voltage and length of the cathode fall. Efficient ionization of the electronegative gas, HCl, which has a low ionization threshold, resulted in an overall contraction of the cathode fall in He mixtures.

20. DISTRIBUTION/AVAILABILITY OF ABSTRACT UNCLASSIFIED/UNLIMITED ☒ SAME AS RPT ☐ DTIC USERS ☐	21. ABSTRACT SECURITY CLASSIFICATION UNCLASSIFIED
22a. NAME OF RESPONSIBLE INDIVIDUAL ACSC/EDCL Maxwell AFB, AL 36112-5542	22b. TELEPHONE NUMBER (Include Area Code) (205)293-2483 22c. OFFICE SYMBOL

DD FORM 1473, 83 APR EDITION OF 1 JAN 73 IS OBSOLETE

UNCLASSIFIED
SECURITY CLASSIFICATION OF THIS PAGE

PREFACE

Understanding the various regions of a glow discharge has led to improvements in a wide variety of military systems, such as high power excimer lasers, thyratrons for high power switches, and plasma reactors for etching or deposition of thin films in the manufacture of semiconductor chips. Many of these discharges of current military interest now contain reactive electronegative gases. It is hoped this manuscript has provided the reader a better understanding of the influence electronegative gases have on the cathode fall region of a glow discharge. This manuscript summarizes the results of a more comprehensive AFIT doctoral dissertation.

I am grateful to Dr. Alan Garscadden, my dissertation advisor at the Aero Propulsion Laboratory, and Major Douglas Deobler, Air Command and Staff College faculty member, for reading this manuscript and providing their critical comments. Special thanks goes to the Aero Propulsion Laboratory Power Division who sponsored this study.

Subject to clearance, this manuscript will be submitted to the Journal of Applied Physics for consideration. The format of the manuscript, including references, are consistent with the requirements for publication in that journal.

ABOUT THE AUTHOR

Major Duke received a Bachelor of Arts Degree in both Physics and Economics from Grinnell College, Iowa, in June 1971. He began his military career at that time after being commissioned a second lieutenant through the Air Force Reserve Officer Training Corps. He attended the University of Missouri-Rolla through an educational delay and received a Master of Science Degree in Physics. He came on active duty in August 1973 and was assigned to the 4000th Aerospace Applications Group (SAC) at Offutt AFB, Nebraska. There he planned and controlled the real-time operations of Defense Meteorological Satellite Program (DMSP) weather satellites. He then attended Squadron Officer School in residence followed by three years at the Air Force Institute of Technology at Wright-Patterson AFB, Ohio. After completing the course requirements for a Doctoral Degree in Physics, he spent four years in the Aero Propulsion Laboratory at Wright-Patterson AFB. As Technical Area Manager of the Plasma Physics Group, he managed basic research in laser diagnostic techniques, high power switches, and plasma processes in deposition devices. He concluded his tour in the laboratory as Executive Officer. Upon completion of his dissertation on sheath phenomena in electronegative glow discharges, he attended the Program Manager's Course at the Defense Systems Management College, Ft. Belvoir, Virginia. He then spent two years at Space Division at Los Angeles AFS, California, developing new environmental sensors and planning the acquisition of the next major satellite redesign for DMSP. Major Duke is presently a member of the Air Command and Staff College class of 1987.

TABLE OF CONTENTS

LIST OF ILLUSTRATIONS

TABLES

FIGURES

EXECUTIVE SUMMARY

Part of our College mission is distribution of the students' problem solving products to DoD sponsors and other interested agencies to enhance insight into contemporary, defense related issues. While the College has accepted this product as meeting academic requirements for graduation, the views and opinions expressed or implied are solely those of the author and should not be construed as carrying official sanction.

"insights into tomorrow"

REPORT NUMBER 87-0730

AUTHOR(S) MAJOR GARY L. DUKE, PhD, USAF

TITLE INVESTIGATION OF SHEATH PHENOMENA IN ELECTRONEGATIVE GLOW DISCHARGES

I. Purpose: To educate the scientific community about how the addition of a gas which easily forms negative ions (electronegative gas) influences the cathode region and thus the voltage drop across a glow discharge. A glow discharge consists of a set of electrodes surrounded by a gas or gas mixture. A fluorescent light is a simple glow discharge operated with an alternating current.

II. Problem: The width of the light and dark regions close to the cathode have been experimentally observed (Ref 8) to contract longitudinally toward the cathode when an electronegative gas was added to a rare (inert) gas discharge. A smaller voltage drop across this region is anticipated as a result of this contraction. Theoretical models constructed to describe electric discharge lasers, high power switches, and devices used to manufacture semiconductors have typically treated the voltage drop across the cathode fall region as a constant, as if the electronegative gas did not affect it. This paper attempts to resolve this inconsistency by explaining why the width of the cathode fall contracts when an electronegative gas is added to the discharge.

III. Data: A theoretical model of the cathode fall region was constructed. The electron kinetics were analyzed by solving the one dimensional, time independent, collisional Boltzmann equation

which describes statistically a swarm of electrons as it traverses the cathode fall region. The only production and loss mechanisms for electrons was assumed to be ionization and attachment. No loss mechanism was assumed to exist for negative ions. This assumption holds for low pressure discharges where ion-ion recombination can be neglected. The positive ion kinetics are based on Poisson's equation which relates the net charge density to a fluctuation in the electric field and an approximation for the mobility of the ions in high electric fields. The negative ion density is derived from the electron kinetics, since the negative ions are formed by slow electron collisions with the electronegative gas molecules. The negative ion mobility is assumed to be the same as the positive ion mobility. This is a good first approximation, but could be refined in a later analysis.

Gas mixtures of helium, argon, and xenon with 1% and 5% hydrochloric acid were analyzed. The electric field, the Townsend ionization and attachment rates, and charged particle densities were calculated as a function of distance across the cathode fall region and compared. A contraction was predicted in the helium mixtures, none was predicted in the argon mixtures, and a slight expansion in the cathode fall was predicted in xenon mixtures.

IV. Conclusions: The results indicated ionization and not attachment of a gas such as hydrochloric acid in helium mixtures led to the contraction and a reduced voltage drop across the cathode fall. Since the ionization threshold of the added electronegative gas was less than the rare gas, less voltage was required to accelerate electrons to achieve the same net ionization in this region. It was also observed that the gas with the lower ionization threshold was spatially ionized first leading to a separation of the gas components in the cathode region. The density of positive ions resulting from electron ionization at the edge of the cathode fall was always found to determine the slope of the electric field in all mixtures.

Conversely, results indicated electron attachment in the cathode fall region increased the cathode fall voltage and length. Although the attachment coefficient was larger than the ionization coefficient immediately in front of the cathode, the

CONTINUED

density of negative ions did not contribute significantly to the space charge until near the end of the cathode fall. The voltage drop and length of the cathode had to increase in order to maintain the same net ionization as occurred in a pure rare gas. The classical theory that the formation of negative ions in the cathode fall causes it to contract due to their slower mobility was shown to be false.

V. Recommendations: Scientists and engineers modeling electric discharge lasers, high power switches, and plasma deposition and etching devices should not assume the voltage drop across the cathode fall region in discharges containing mixtures is equivalent to the voltage drop across the cathode fall region of a discharge containing the primary constituent (usually the rare gas). The voltage drop across the cathode fall can be significantly affected by trace species if their threshold for ionization is less than the primary constituent. Scientists modeling plasma deposition and etching devices should also be aware that the gases are sequentially ionized across the cathode fall region in order of their ionization thresholds. This phenomena could impact the uniformity and reproducibility of their films.

I. INTRODUCTION

Previous papers have analyzed the cathode fall in electropositive glow discharges.[1, 2, 3, 4, 5, 6, 7] This paper analyzes the cathode fall in an electronegative glow discharge. An understanding of the formation of positive and negative ions in electronegative glow discharges is very important in modeling electric discharge lasers, high power switches, and the plasma in plasma etchers and reactors for depositing thin films. In 1938, Emeleus and Sayers[8] reported the width of the luminous and dark regions in the cathode fall and negative glow region of a helium discharge contracted significantly towards the cathode with the addition of just a trace of chlorine, an electronegative gas. This contraction of the cathode fall implies a decrease in cathode fall voltage. This change in voltage is important because it determines the energy of the electrons and ions which traverse the cathode fall region and enter the negative glow. This paper explains the contracted cathode fall region observed in electronegative glow discharges.

Two theoretical approaches exist for calculating the nonequilibrium electron energy distribution function in the cathode fall region of a glow discharge. The Monte Carlo method is based upon the statistics of modeling a large number

(typically 10^5 or greater) of electron collisions with gas molecules in the presence of an electric field.[3, 7, 9] The other method is based upon numerically solving the time independent Boltzmann equation for the electron distribution function. In uniform electric fields, agreement between these methods has been excellent.[10, 11, 12] Allis and co-workers[1, 2] and Long[5] assumed a linearly decreasing electric field through the cathode fall and used the Boltzmann method to model the change in the electron distribution function as a function of distance. Tran Ngoc, et al.[7] and Segur[3] similarly assumed a linearly decreasing electric field, but used the Monte Carlo model. These calculations are not considered self-consistent. The perturbation of the electric field from electron nonequilibrium kinetics, which their calculations showed had occurred in the cathode fall region, was not examined. Since then Segur et al.[6] have coupled a Boltzmann solution for electrons with an analytical approximation to the Boltzmann equation for positive ions in the cathode fall region in a self-consistent manner for various helium-mercury mixtures. Boeuf et al.[4] investigated the cathode fall in a helium discharge using a self-consistent Monte Carlo technique, which sequentially iterated Monte Carlo calculations for positive ions followed by a calculation of the electric field, and then another Monte Carlo calculation for electrons. The present paper is based on the Boltzmann technique derived by Allis et al.[2] and Long[5], and modified to include the formation of negative ions as well as a self-consistent calculation of the electric field.

II. MODELING

a. Theory

The cathode fall region is assumed to be a weakly ionized, collision dominated, nonneutral plasma consisting of four components: electrons, positive ions, negative ions, and neutrals. The densities of negative and positive ions are derived from the negative ion current density and current conservation respectively. The neutral density is assumed to remain constant.

The electron density and the electron energy distribution are determined by numerically solving the time independent, one dimensional, collisional Boltzmann equation. This representation models the distribution f of a swarm of electrons as it traverses the cathode fall of a glow discharge. The one dimensional Boltzmann equation

$$v_x \frac{\partial f}{\partial x} + \frac{e}{m} E(x) \frac{\partial f}{\partial v_x} = \frac{\partial f}{\partial t}\Big)_{col} \qquad (1)$$

is transformed into energy space as

$$\frac{\partial f}{\partial \phi} + \frac{\partial f}{\partial \xi} = \frac{1}{e v_x E(x)} \frac{\partial f}{\partial t}\Big)_{col} \qquad (2)$$

where $\phi = e\int E(x)dx$ is the electron potential energy and $\xi = mv_x^2/2$ is the electron kinetic energy induced by the electric field E(x). Let the total electron kinetic energy be represented by $\varepsilon = \xi + \eta$

where ε is the random or thermal energy contribution. The distribution function f can then be represented as the sum of two functions, $f_-(\varepsilon,\xi,\phi)$, which is the distribution of electrons with $v_x < 0$ moving against the field and $f_+(\varepsilon,\xi,\phi)$, which represents those electrons with $v_x > 0$ moving with the field. The right hand term represents the change in f due to the collision processes in the gas. This equation subsequently is transformed into a linear integral operator equation.[13]

$$\frac{\partial f}{\partial \phi} + \frac{\partial f}{\partial \varepsilon} = \frac{1}{e E_N(\phi)} \left(\frac{\varepsilon}{\xi}\right)^{\frac{1}{2}} \left[K - Q(\varepsilon)\right] f \qquad (3)$$

where K is an integral operator representing a sum over all collisional processes, $Q(\varepsilon)$ is the total electron cross section, and N is the gas density. Derivation of the individual operators for each electron collisional process can be found in Long's report.[5]

The collisional term is further simplified by assuming Kf to be nearly isotropic in velocity space and expanding Kf in Legendre polynomials. This expansion differs from the usual two term expansion[1] of Boltzmann's equation in spherical harmonics in that it is an expansion of the product of the integral operator times f, not an expansion of f. The resulting equation is solved numerically using an iterative technique developed by Long[5]. It is assumed initially that electrons are only scattered-out of each element of velocity space (Kf=0). The equation is then integrated for both forward and backward moving electrons.

Scattered-out electrons then become scattered-in electrons for other elements of velocity space. This gives a first approximation to the electron distribution function from which a new operator Kf is calculated. This procedure was repeated until convergence was reached (taken as less than .2% change in the distribution function). For a 200 eV cathode fall, the energy resolution of the calculation corresponded approximately to 1 eV.

From the electron energy distribution, the electron number density, electron current density, and Townsend ionization coefficient were calculated. The electron energy and number density distributions were normalized to the distribution at the cathode. In order to obtain a completely self-consistent solution in which Poisson's equation is obeyed in addition to boundary conditions at the cathode and anode, successive calculations for the electron distribution function, electron number density, and resulting electric field were accomplished.

The electric field is obtained by putting Poisson's equation in difference form so the value of the field at each point is based on the value at the previous increment with the field at the cathode given as a boundary condition.

$$E_j = E_{j-1} - \frac{e}{\varepsilon_0}\left[n_{+j} + n_{+j-1} - n_{ej} - n_{ej-1} - n_{-j} - n_{-j-1}\right]\frac{(x_j - x_{j-1})}{2} \qquad (4)$$

where n_{+j}, n_{ej}, and n_{-j} are the positive ion, electron, and negative ion densities at position j, and x_j is the spatial point corresponding to increment j. The positive ion density is

written in terms of the current conservation (J = total current density) using Ward's modified formula[14] for the ion drift velocity for high field regions.

$$n_{+j} = \frac{(J - j_{ej} - j_{-j})}{e\, k_+ \left(\frac{E_j}{p}\right)^{\frac{1}{2}}} \qquad (5)$$

where j_{ej} and j_{-j} are the electron and negative ion current densities at location j. Similarly the negative ion density is calculated by dividing the negative ion current density by its velocity (k_- is assumed to be equal to k_+).

$$n_{-j} = \frac{J_-}{e\, k_- \left(\frac{E}{p}\right)^{\frac{1}{2}}} \qquad (6)$$

Since the negative ions are formed as a result of electron attachment, the negative ion current density is obtained by integrating over all attaching collisions.

$$J_- = \int_0^x \beta_j\, j_{ej}\, dx_j \qquad (7)$$

where is the attachment rate. Equation 4 then becomes a fifth order polynomial whose roots were found numerically using Steinman's method.[15] The lowest real value of E (some are imaginary) at the cathode boundary was picked as the solution, since it led to the lowest possible cathode fall voltage. The electric field at each location is therefore calculated from n_e, j_e, j_- and the value of the electric field at the previous

spatial increment. This technique converged quickly, normally within 4-6 iterations for three significant figure convergence.

b. Gas and Discharge Parameters

The gas and discharge parameters used in the calculations are summarized in Table 1. For a required electron energy resolution of 1 eV, the electrode distance (D) was limited by the memory storage capability of a Cyber 74 computer. For 100% He, D was 2.2 cm and for the remaining He/HCl mixtures, it was 2.1 cm due to the contraction that occurred. γ is the secondary electron emission coefficient of the cathode for ion bombardment. The distribution of electrons leaving the cathode was the same as that used by Long[5] (16% between 1-2 eV, 25% between 2-3 eV, 28% between 3-4 eV, 25% between 4-5 eV, and 6% between 5-6 eV). The mobility, k_+, of the positive ions was represented by those of the rare gases.

Table I. Gas and discharge parameters used in the Boltzmann calculations.

Mixtures	D (cm)	J (amp/cm^2)	γ	k $\frac{\text{cm-torr}}{\text{volt-sec}}$
He/HCl	2.1-2.2	16	.2	4.1E+4
Ar/HCl	1.15	10	.0417	8.25E+3
Xe/HCl	.87	10	.004	4.0E+3

c. Electron Impact Cross-Sections.

The cross-sections used for He, Ar, Xe, and HCl in the Boltzmann calculations are shown in Figs. 1-5. Thresholds and

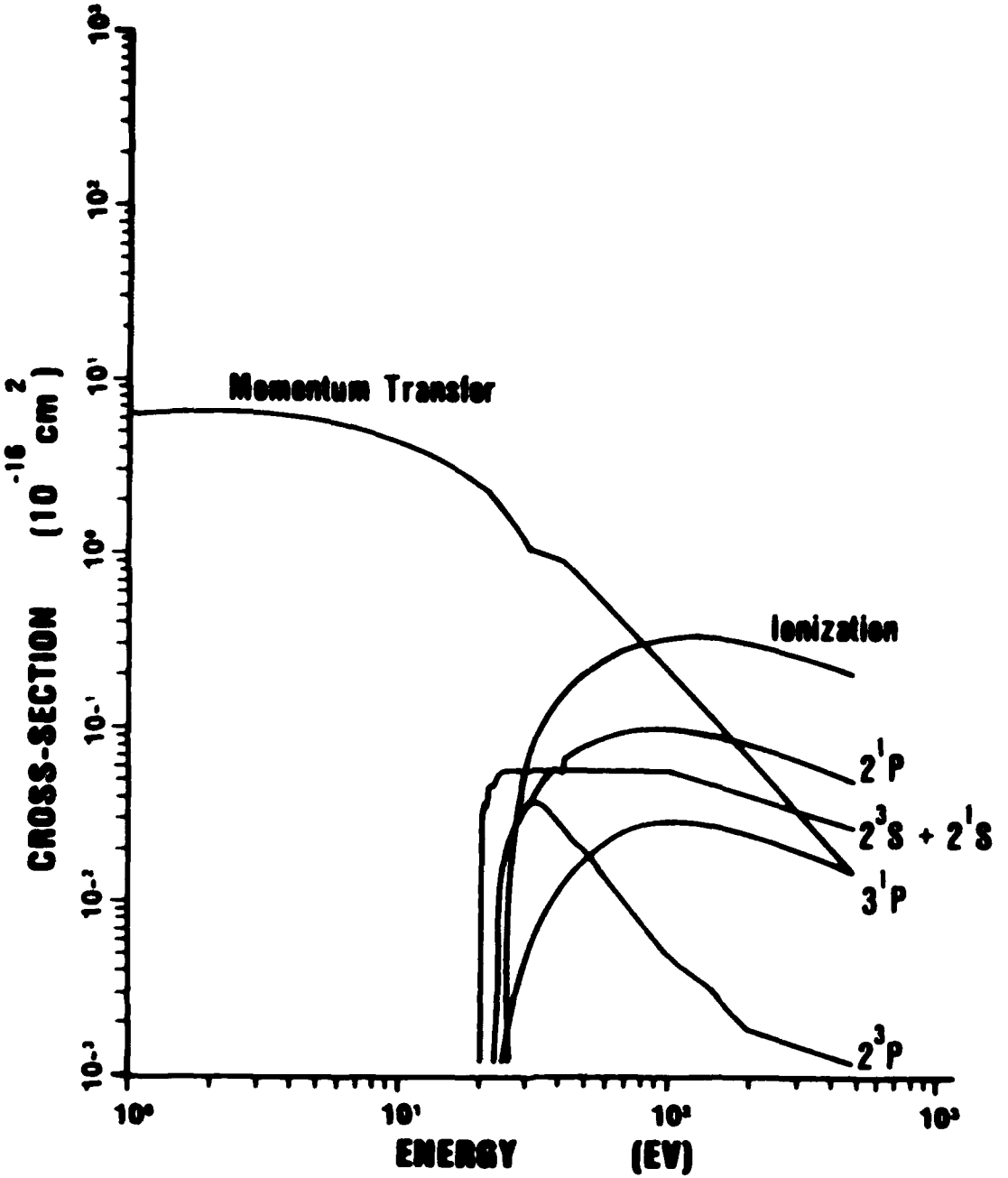

Figure 1 ELECTRON IMPACT CROSS SECTIONS IN He.

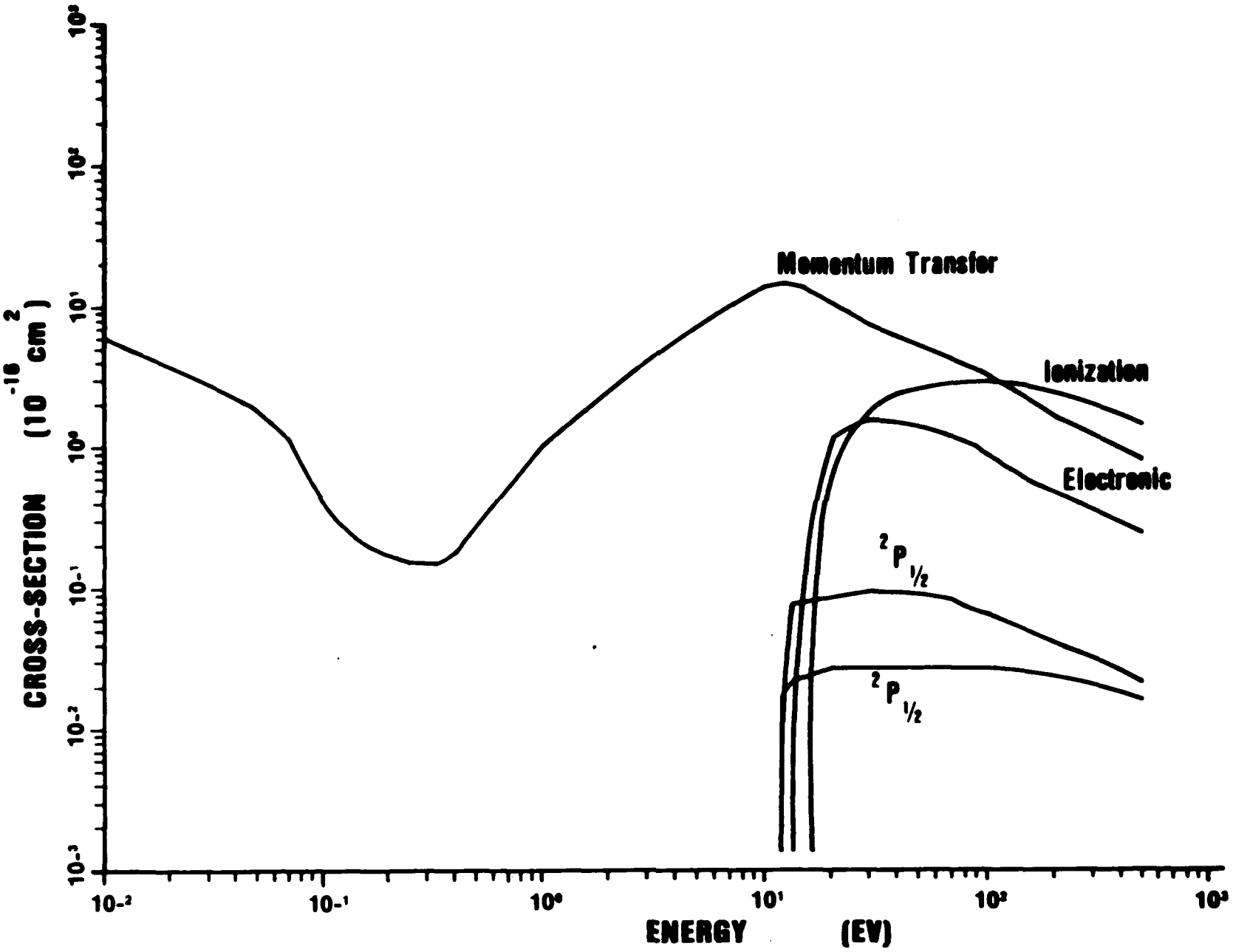

Figure 2 ELECTRON IMPACT CROSS SECTIONS IN Ar.

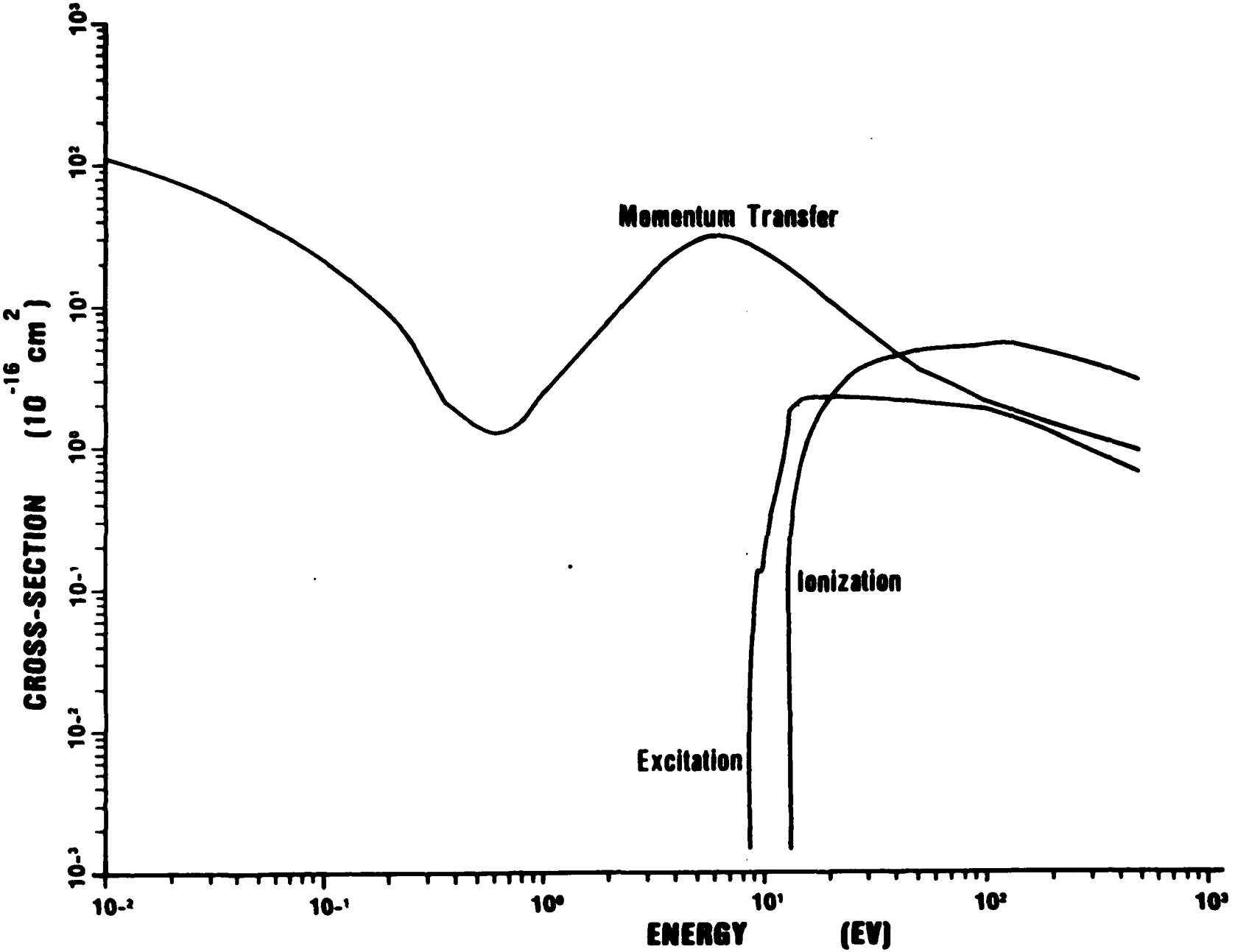

Figure 3 ELECTRON IMPACT CROSS SECTIONS IN Xe.

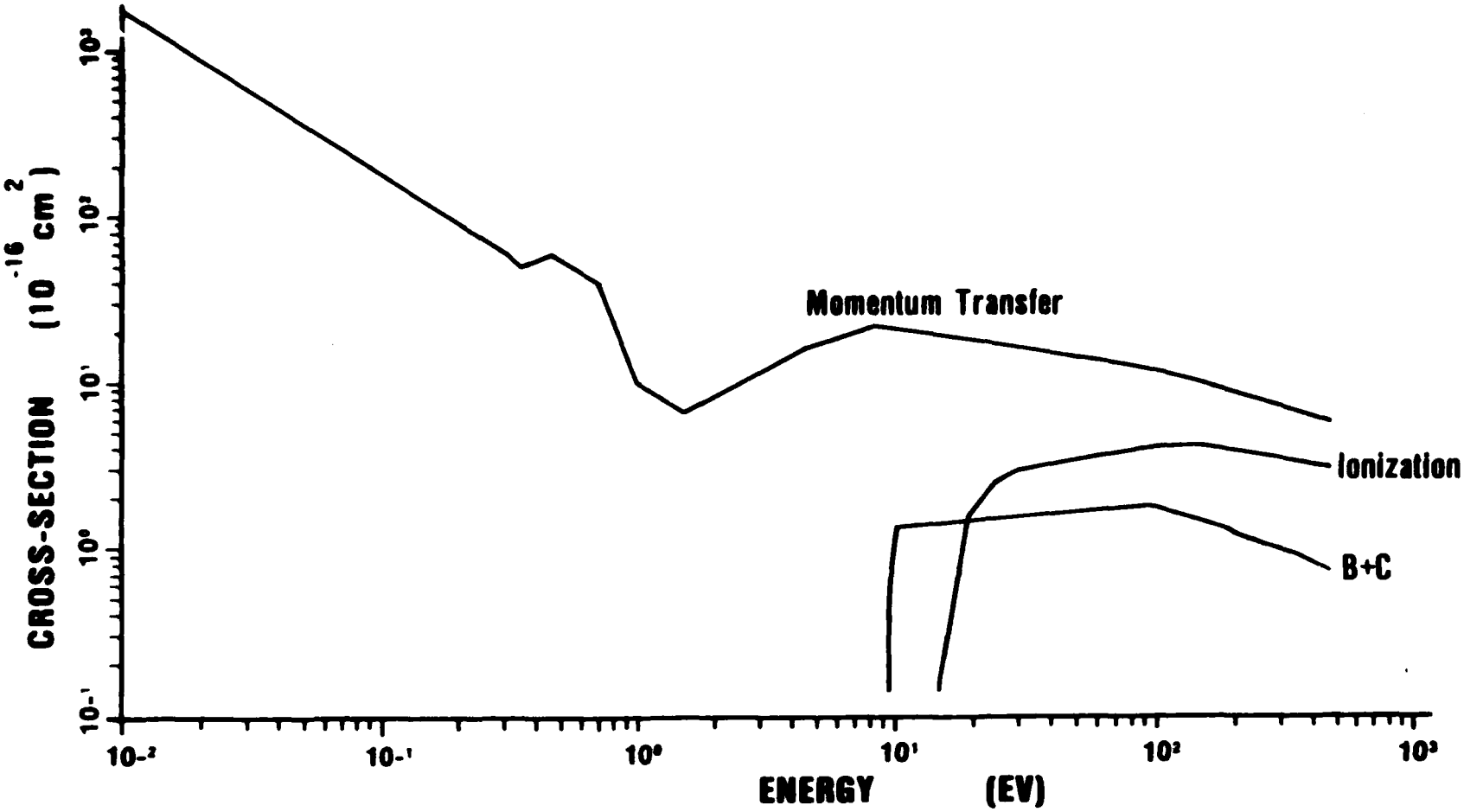

Figure 4 HIGH ENERGY ELECTRON CROSS SECTIONS IN HCl.

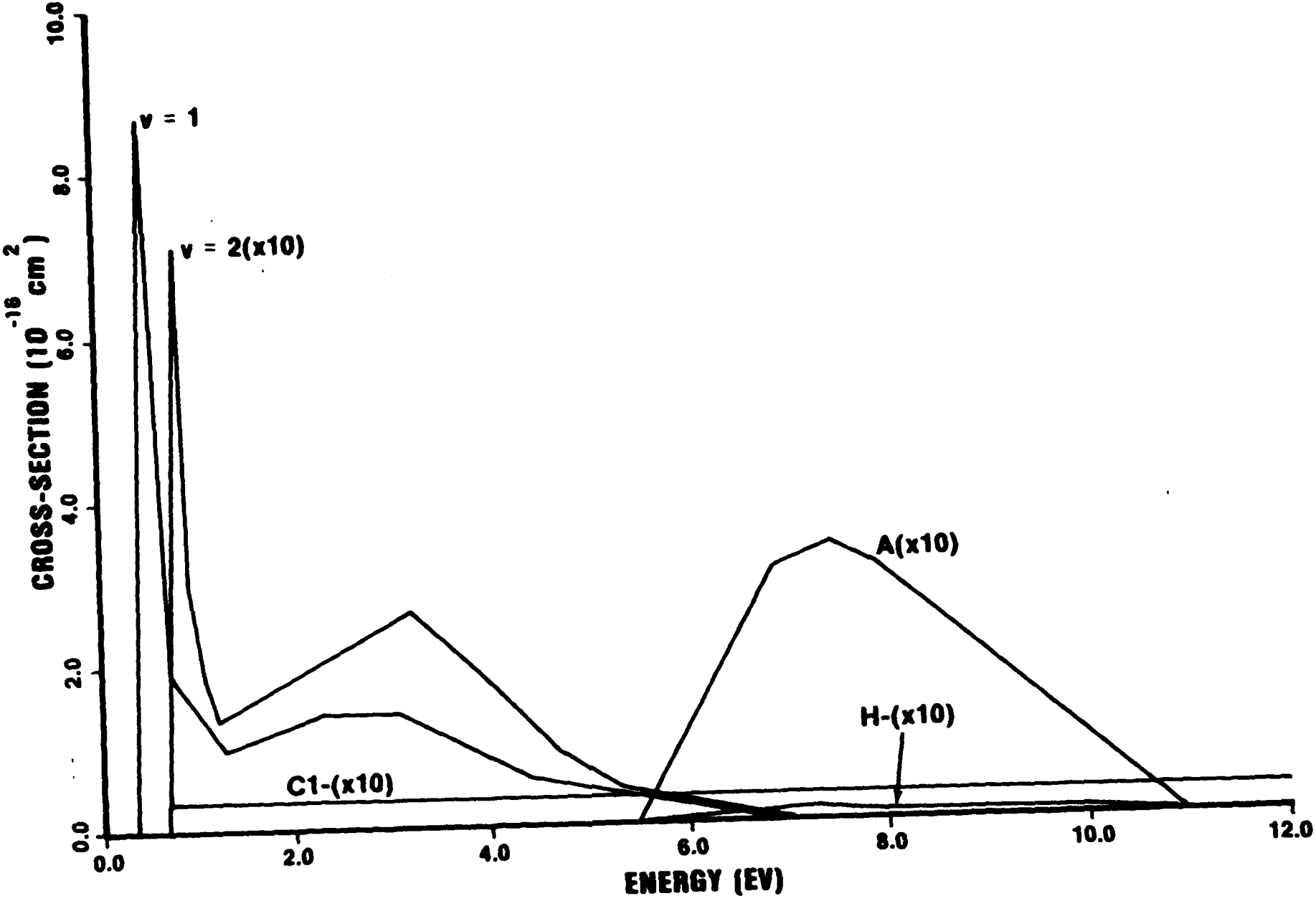

Figure 5 LOW ENERGY ELECTRON CROSS SECTIONS IN HCl.

references for each energy range are listed in Table II. The most important cross sections in the calculations are the ionization cross sections of the rare gases. This cross section determines how quickly the electrons multiply, and thus directly effects n_e and dE/dx in Poisson's equation. For the rare gases, the ionization cross section was obtained from measurements by Rapp et al.[16] over the complete energy range. The ionization cross section for HCl had to be extended above 100 eV. Since HCl was used in small concentrations and the mean electron energy in the HCl mixtures was always less than 87 eV, any error in the approximation should be negligible. Electronic cross sections for He were extended using the formulas listed under the reference column in Table II.

III. DISCUSSION

The theory described above was used to model the cathode fall in He/HCl, Ar/HCl, and Xe/HCl mixtures. All data presented was obtained for a gas pressure of 1 torr at a temperature of 300 K. Gas and discharge parameters previously described in Table I were held constant. The only production and loss processes for electrons was assumed to be ionization and attachment. At low gas pressures ion-ion recombination can be neglected. No loss process for negative ions was assumed to exist.

Table II. Thresholds for electron impact cross sections.

Process	Range (eV)	References
He		
Momentum	0.-6.	17
Transfer	6.-500.	18
Electronic		
$2^3S \rightarrow 2^1S$	19.81-23.54	17
	24.-100.	Constant
	100.-500.	$\sigma = .624/\varepsilon^{\frac{1}{2}}$
2^3P	20.95-199.6	17
	200.-500.	$\sigma = .02755/\varepsilon^{\frac{1}{2}}$
2^1P	21.2-196.1	17
	200.-500.	$\sigma = 1.179/\varepsilon^{\frac{1}{2}}$
3^1P	23.07-207.8	17
	210.-500.	$\sigma = .3605/\varepsilon^{\frac{1}{2}}$
Ionization	24.59-500.	16
Ar		
Momentum	0.-30.	17
Transfer	30.-500.	5
Electronic		
$^2P_{3/2}(3p^5)$	11.6-500.	19
$^2P_{1/2}(2p^5)$	11.8-500.	19
Remaining	13.2-500.	19
Ionization	15.76-500.	16
Xe		
Momentum	0.-6.5	17
Transfer	6.5-20.	19
	20.-500.	18
Electronic	8.32-500.	19
Ionization	12.13-500.	16
HCl		
Momentum	0.-100.	20
Transfer	100.-500.	Log Extrapolation
Vibration		
v = 1	.36-7.	20
v = 2	.7-7.2	20
Attachment		
Cl^-	.67-2.7	20
H^-	5.6-12.	20
Excitation		
A	5.5-11.	20
B + C	9.3-100.	20
	100.-500.	19
Ionization	12.74-100.	20
	100.-500.	19

a. Helium mixtures

A 15% decrease in the electric field is predicted as the amount of HCl is increased from 0 to 5% in Fig. 6. This corresponds to a 32% decrease in cathode fall voltage and a 21% decrease in cathode fall length. This decrease in voltage and distance as a function of HCl is due to the increase in the Townsend ionization coefficient, as displayed in Fig. 7. This increase in ionization in the peak region occurs because HCl is much easier to ionize than He (the ionization threshold for HCl is 12.74 eV, versus 24.59 eV for He). Also, the spatial threshold for the Townsend ionization coefficient is halved when HCl is added, reflecting the change in threshold for ionization. Thus very close to the cathode, more HCL is being ionized than He. This is consistent with the results of Segur, et al.[6] with Hg in He.

The slope of the electric field near the cathode is described by Poisson's equation. As will be seen in later figures, the positive ion density near the cathode is much larger than other charged particle densities by several orders of magnitude. The linear slope of the electric field thus depends only on the near constant value of the positive ion density. The curves in Fig. 6 are thus almost parallel. The electric field curves are shifted down because less voltage is required to produce the same net ionization.

Townsend ionization and attachment coefficients are compared in Fig. 8 as a function of distance for 99/1 and 95/5 concentra-

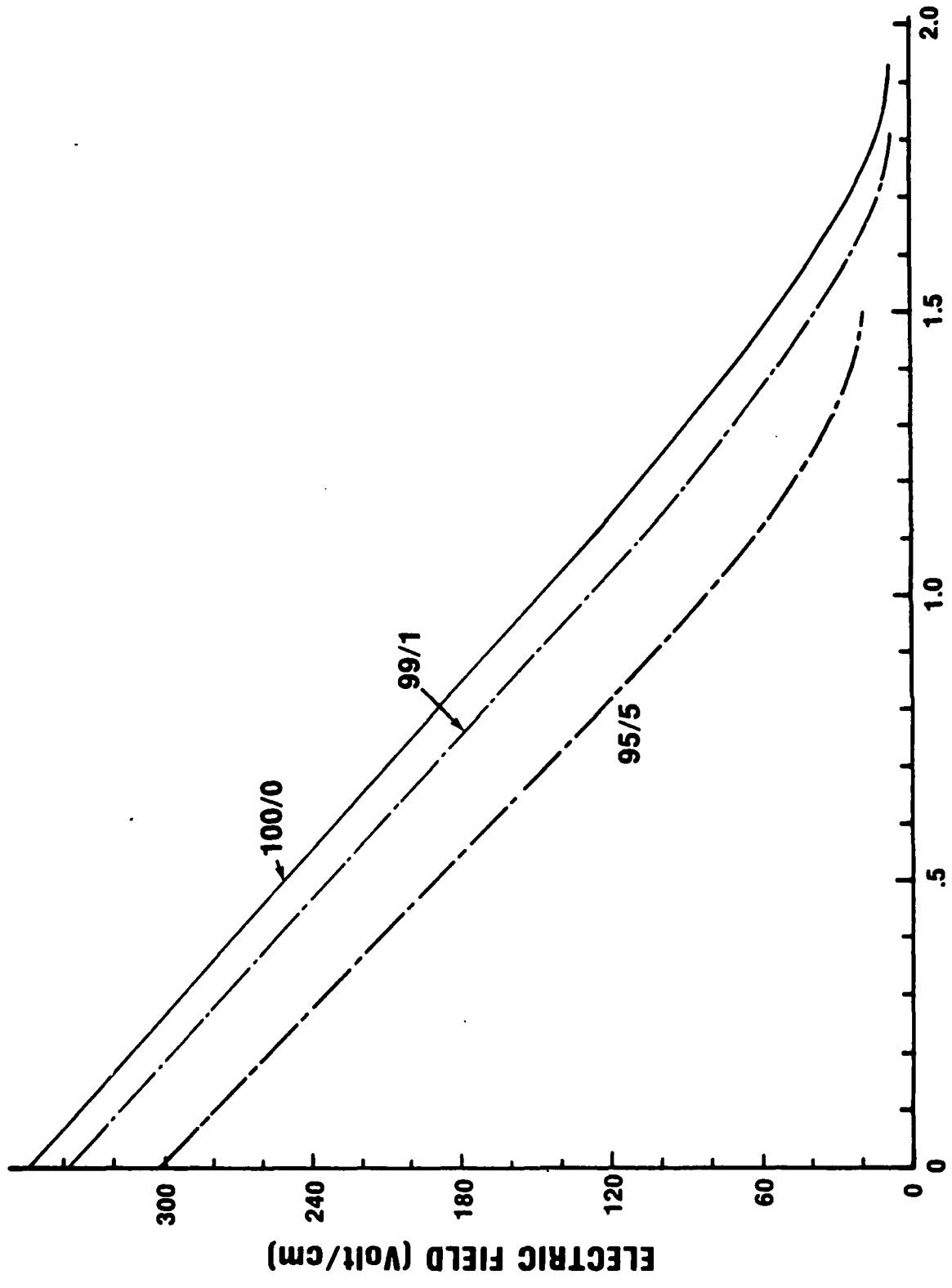

Figure 6 ELECTRIC FIELD IN He/HCl MIXTURES.

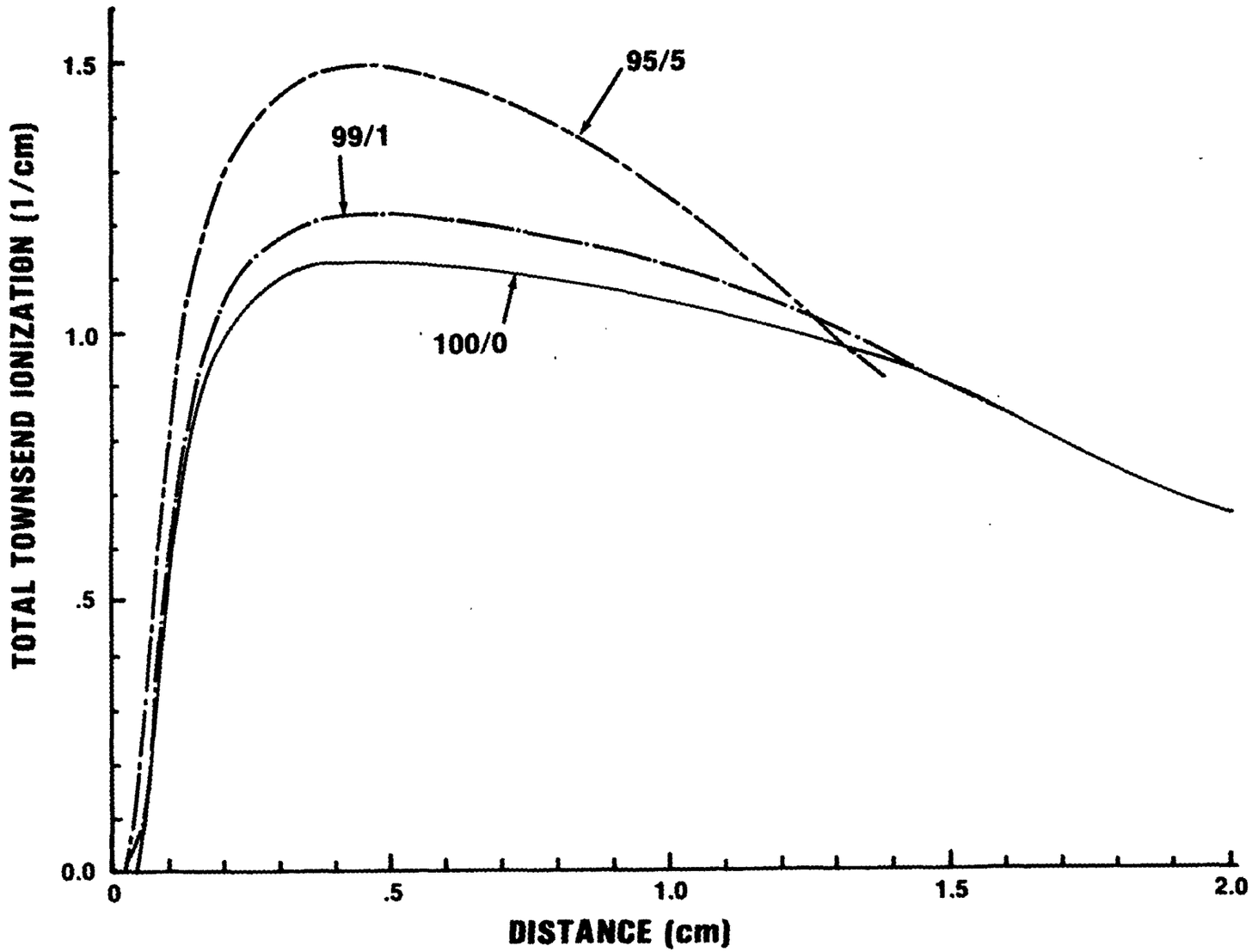

Figure 7 COMPARISON OF TOWNSEND IONIZATION COEFFICIENTS IN He/HCl MIXTURES.

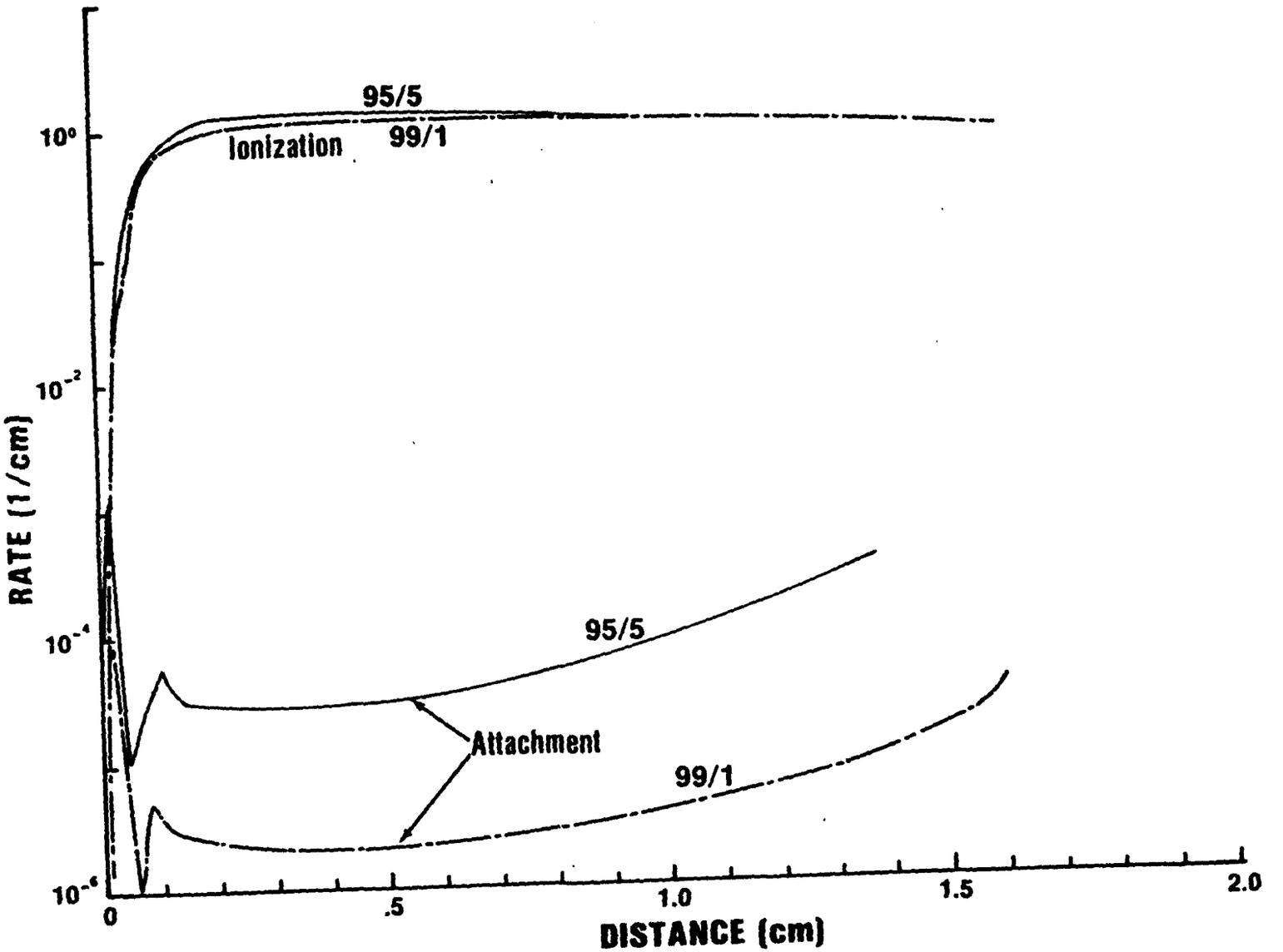

Figure 8 COMPARISON OF IONIZATION AND ATTACHMENT COEFFICIENTS IN He/HCl MIXTURES.

tions of He/HCl. As one would expect, the magnitude of the attachment rate is much smaller than the ionization rate throughout the cathode fall region, except immediately in front of the cathode. In this region, which corresponds to the Faraday dark space, electrons have just left the cathode with a few eV of energy and are more susceptible to attachment than after they have been accelerated to higher energies. The second peak seen in the attachment curve at 1 cm is probably due to the electron distribution function first reaching the ionization energy and producing a new crop of slow secondary electrons. This is consistent with the peak in the ionization coefficient which occurs near the same location.

The electron, positive ion, and negative ion number densities are displayed as a function of distance through the cathode fall region in Fig. 9. The electron density initially decreases because the majority of electrons are rapidly accelerated away from the cathode. Just before they have gained sufficient energy for ionization, their density reaches a minimum. The electron density begins to increase after the ionization potential of the gas is attained. Similarly, the positive ion density increases slightly leaving the cathode because very little ionization occurs close to the cathode as the positive ions are being accelerated towards it. Although negative ions are present throughout the cathode fall region, their density is generally much too small to affect the net space charge to any significant degree. Even in the 95/5 mixture the

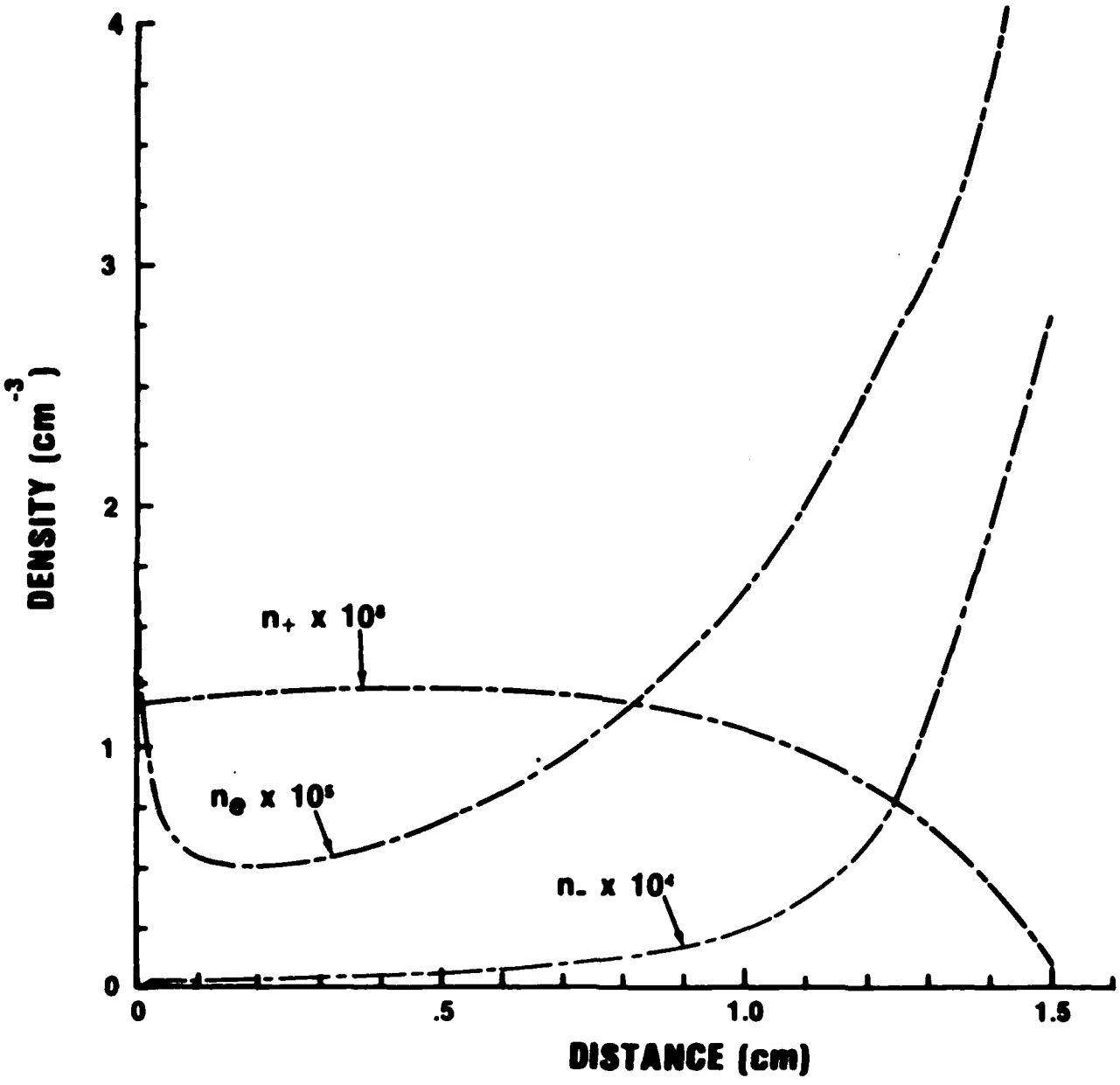

Figure 9 CHARGED PARTICLE DENSITIES IN A 95/5 He/HCl MIXTURE.

negative ion density was still more than an order of magnitude less than the electron density and is more than four orders of magnitude smaller than the positive ion density. The magnitude of the electron density approaches the positive ion density only near the cathode fall-negative glow boundary. Equilibrium was never reached in these examples because a slightly bimodal electron distribution still existed at this boundary.

b. Argon mixtures

In contrast to He mixtures, there is a negligible effect on the electric field in the cathode fall region when up to 5% HCl is added to Ar as shown in Fig. 10. This electric field distribution through the cathode fall corresponds to about a 184 v potential drop across the cathode fall. With 1% HCl, the difference in total ionization is too small to have any observable effect on the electric field. Ionization thresholds for Ar (15.7 eV) and HCl (12.7 eV) are much closer than for He and HCl.

This difference is also too small to be observed in Fig. 11 in the Townsend ionization coefficient. With 5% HCl, there is sufficient HCl to increase the ionization rate about 1.6% throughout most of the cathode fall region. Townsend ionization and attachment coefficients for 99/1 and 95/5 concentrations in Ar/HCl are also compared in this figure. As in He/HCl mixtures, the attachment rate is larger than the ionization rate only for a few electron collisions close to the cathode where the electrons have insufficient energy for ionization.

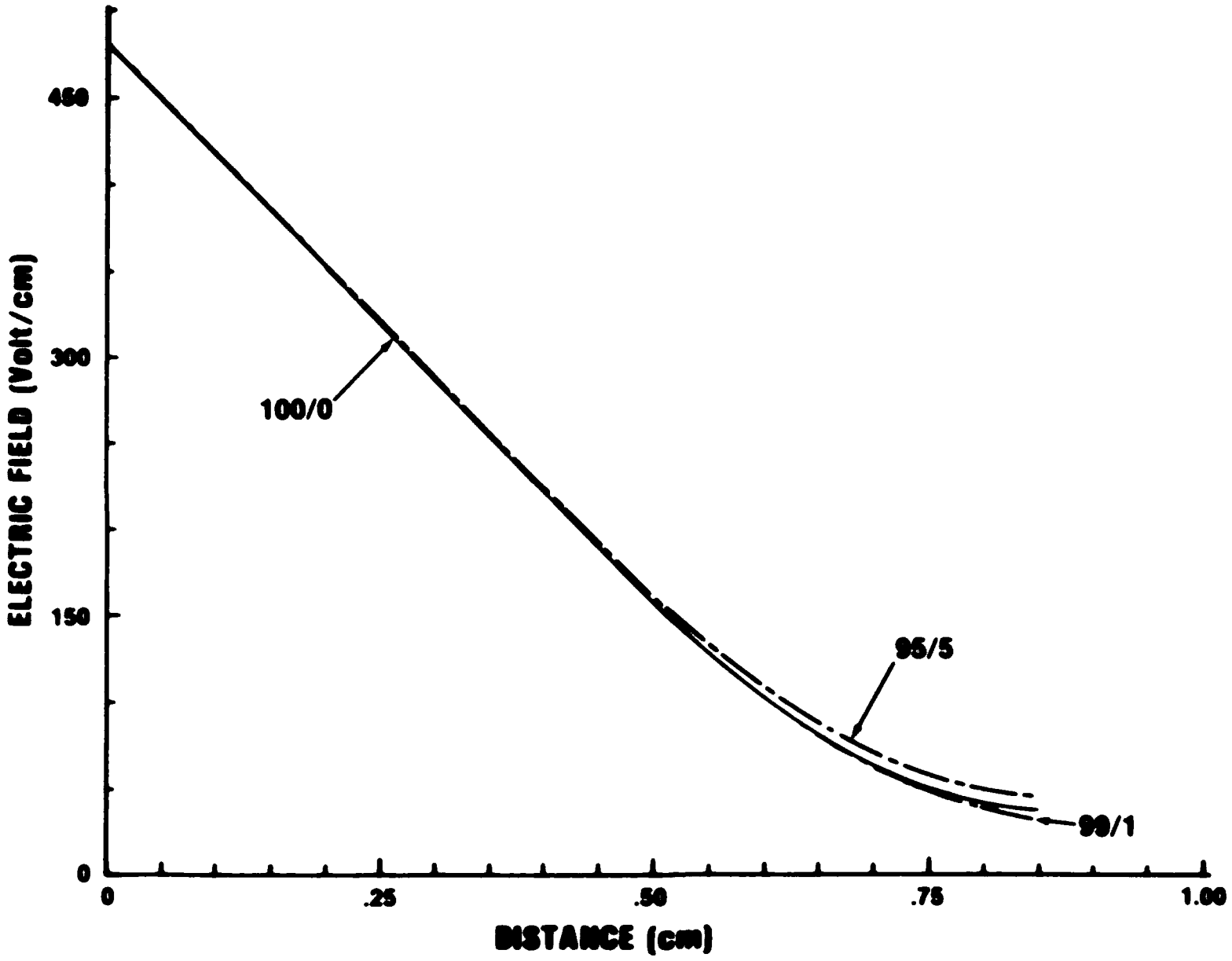

Figure 10 ELECTRIC FIELD IN Ar/HCl MIXTURES.

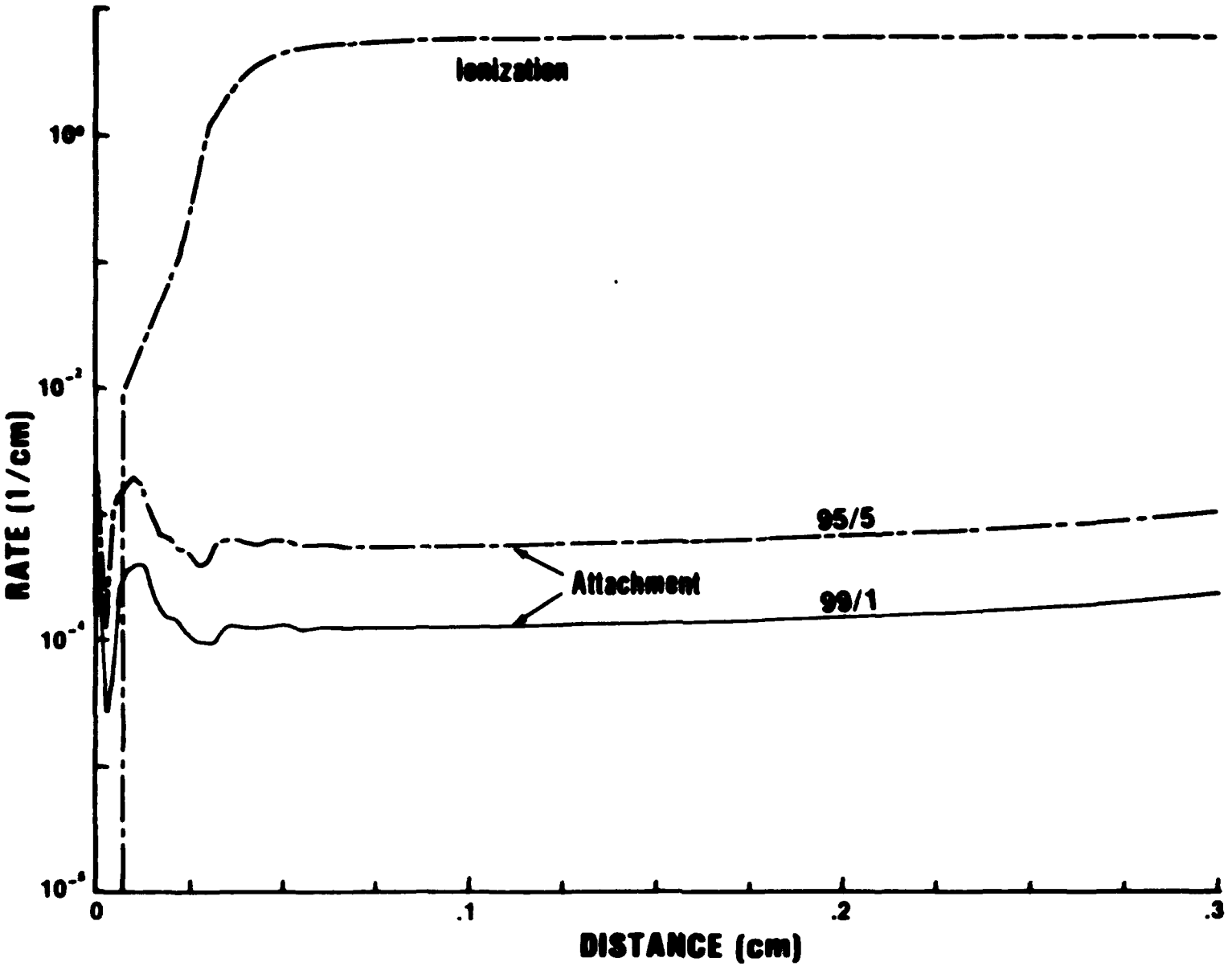

Figure 11 COMPARISON OF IONIZATION AND ATTACHMENT COEFFICIENTS IN Ar/HCl MIXTURES.

The same nonequilibrium phenomena that occurred in number densities in He mixtures is observed in Ar mixtures in Fig. 12. The positive ion density increases in the direction moving away from the cathode, while the electron number density initially decreases. The number of negative ions is more than two orders of magnitude smaller than the number of positive ions, and actually their density does not begin to grow exponentially until the cathode fall begins to merge into the negative glow. The positive ion density is still several orders of magnitude larger than the electron and negative ion densities and thus determines the slope of the electric field.

c. Xenon mixtures

In contrast to He and Ar mixtures, there is a slight increase in the electric field in the cathode fall region when up to 5% HCl is added to Xe as shown in Fig. 13. Slightly higher fields are required to obtain the same net ionization near the cathode due to the formation of negative ions very close to the cathode as well as the additional energy losses to HCl vibrational processes. Xe/HCl mixtures are unique in that both constituents have almost the same ionization potential (12.74 eV for HCl and 12.13 eV for Xe). A loss of electrons close to the cathode is similar to the effect of reducing the secondary emission coefficient of the cathode. A decrease in γ similarly results in a higher cathode fall voltage. However, the slope of the electric field stays the same because positive ions still

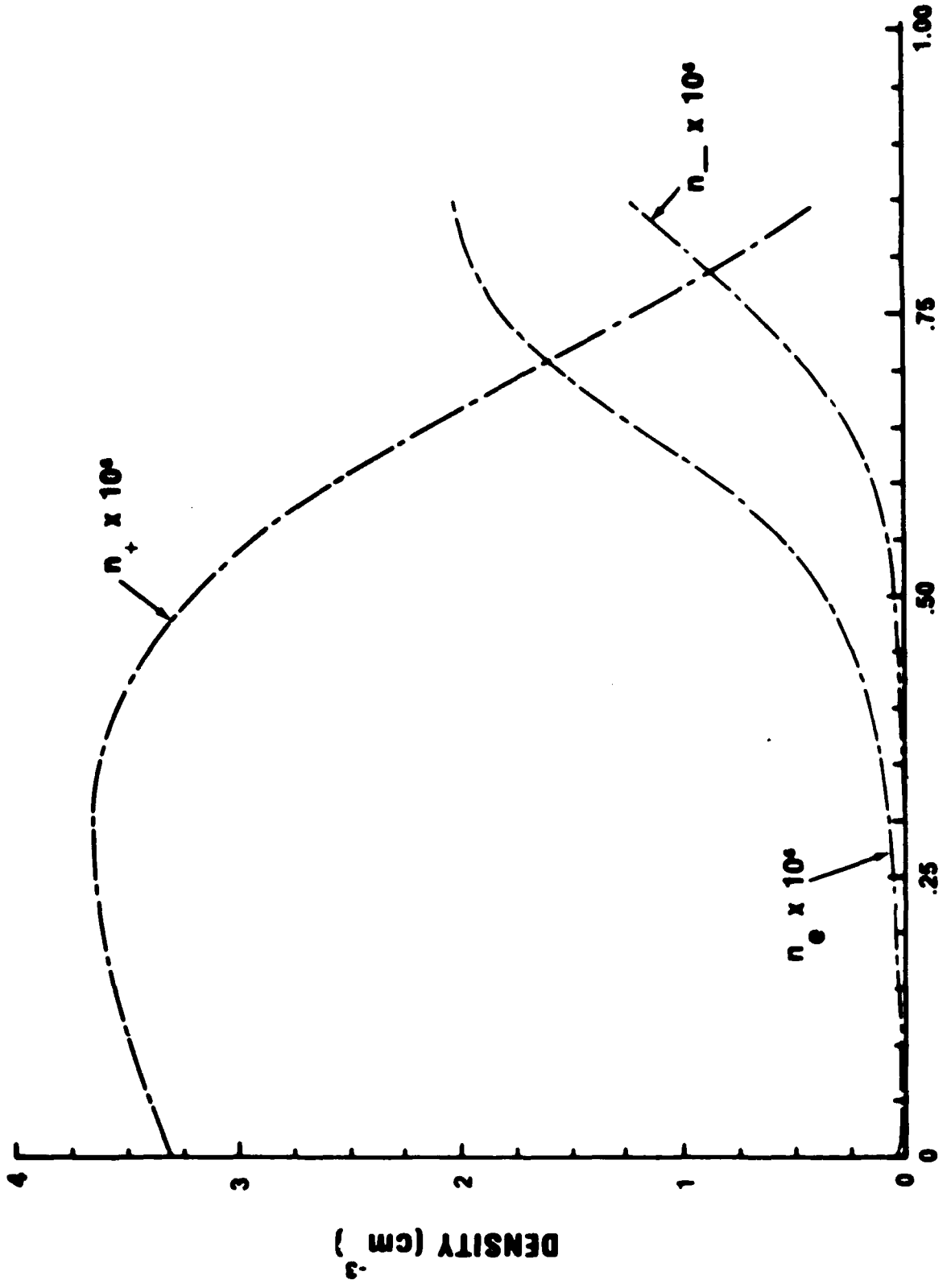

Figure 12 CHARGED PARTICLE DENSITIES IN A 95/5 Ar/HCl MIXTURE.

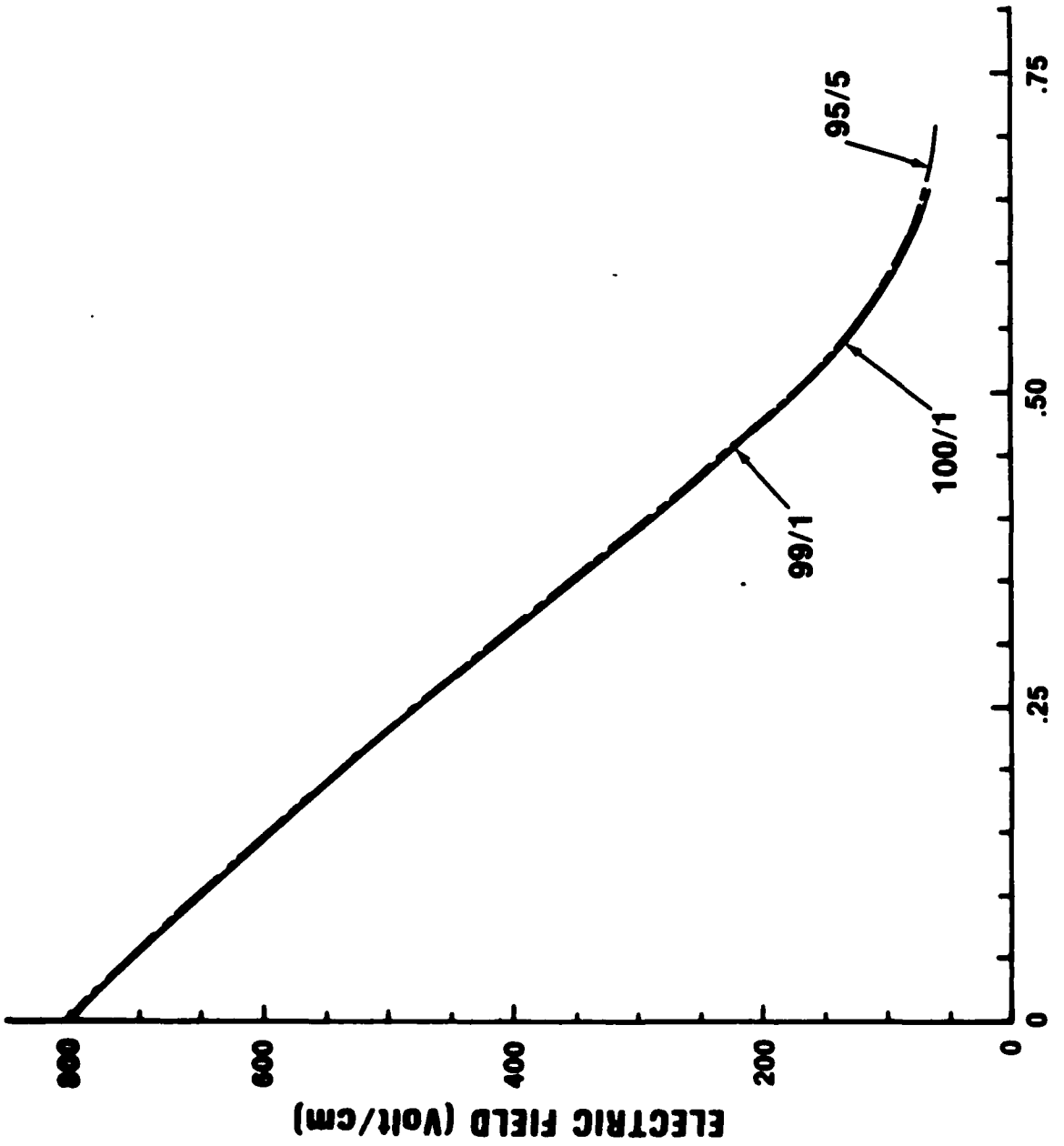

Figure 13 ELECTRIC FIELD IN Xe/HCl MIXTURES.

dominate the other number densities. Thus the trend of the electric field shifting vertically with a corresponding increase in voltage would be expected to continue for larger concentrations of HCl in Xe. In this study the positive ion velocity of only the rare gas was included. Addition of HCl with its higher mobility would increase the average positive ion drift velocity. This would result in a shallower slope of the electric field and a further expansion in cathode fall length.

Townsend ionization and attachment coefficients are compared in Fig. 14 for 99/1 and 95/5 concentrations in Xe/HCl. Again the attachment coefficient is much smaller than the ionization rate throughout the cathode fall region except immediately in front of the cathode. Note that the region where the attachment coefficient is greater than the ionization rate is smaller in Xe mixtures than in either He or Ar mixtures (Figs. 8 and 11 respectively). The onset of ionization however still occurs close to the second peak of the attachment rate.

The nonequilibrium phenomena occurring in the previous rare gas mixtures is also observable in the number densities in Xe mixtures. Results are illustrated in Fig. 15. The trends are similar to those seen in Figs. 9 and 12.

IV. SUMMARY AND CONCLUSIONS

These results indicate ionization and not attachment of a gas such as HCl in He mixtures leads to a contraction and a

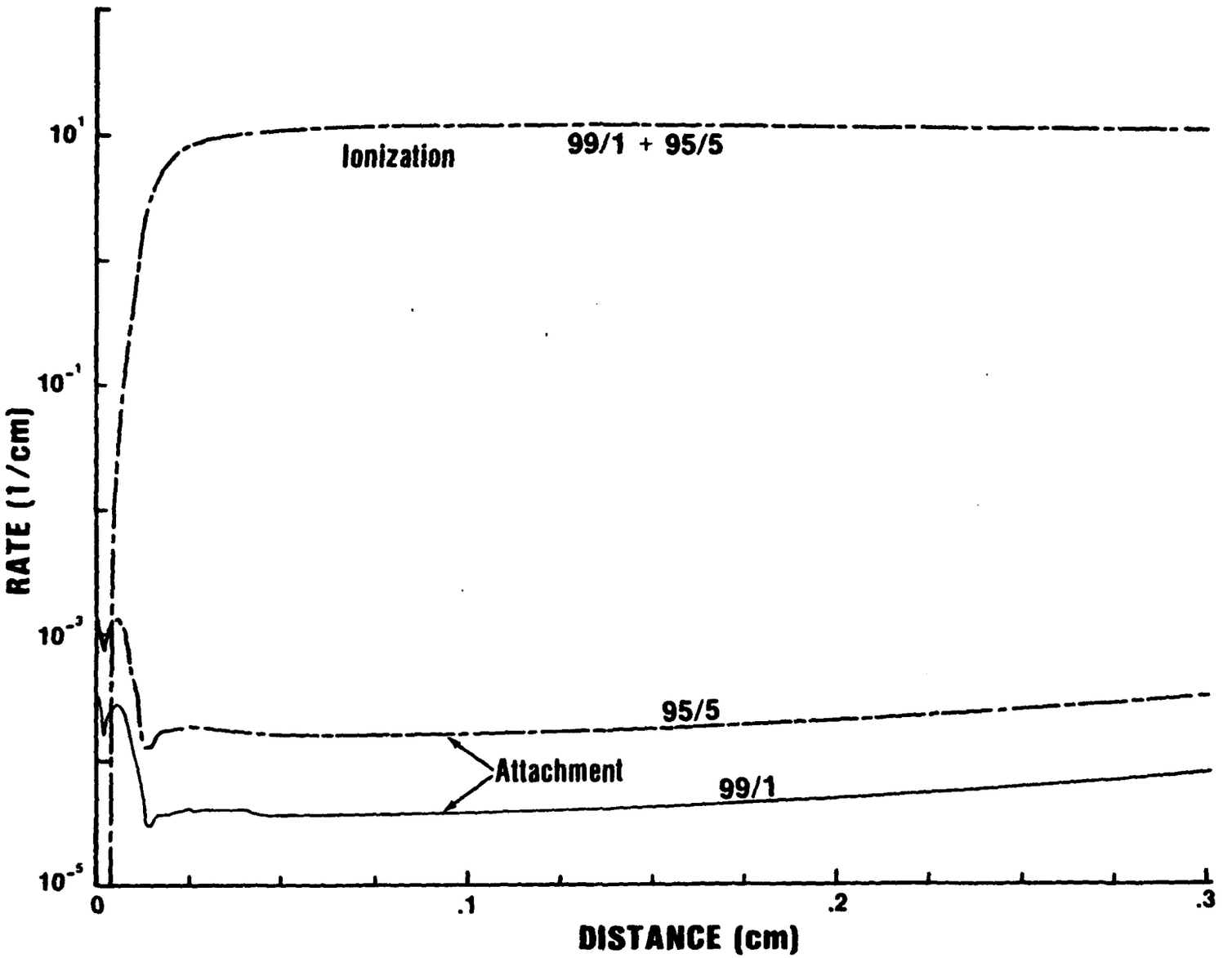

Figure 14 COMPARISON OF IONIZATION AND ATTACHMENT COEFFICIENTS IN Xe/HCl MIXTURES.

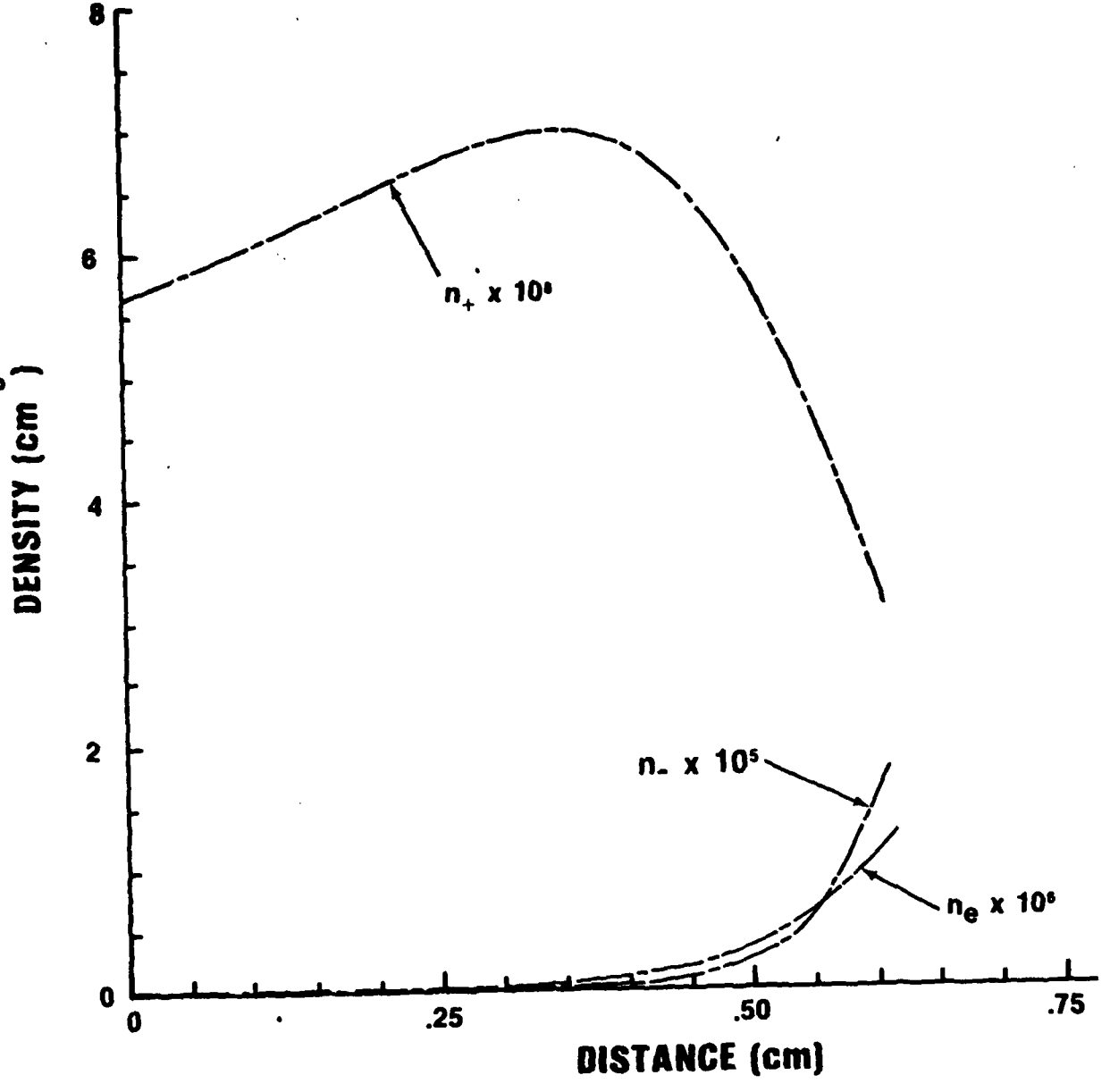

Figure 15 CHARGED PARTICLE DENSITIES IN 95/5 Xe/HCl MIXTURE.

reduced voltage drop across the cathode fall. Since the ionization threshold of the added electronegative gas was less than the rare gas, less voltage was required to accelerate electrons to achieve the same net ionization in the this region. This explains the contraction of the cathode fall region observed by Emeleus and Sayers[8] in electronegative gas mixtures. It was also observed that the gas with the lower ionization threshold was ionized first. This leads to a separation of the gas components in the cathode fall region. Discharge models which include the cathode fall voltage in their circuit analysis should include the different ionization rates and distinct mobilities for each gas species in determining their cathode fall voltage. The density of positive ions was always much larger than the density of electrons and negative ions and thus determined the slope of the electric field in accordance with Poisson's equation as well as the voltage across the cathode fall.

Conversely, results indicated electron attachment in the cathode fall region increased the cathode fall voltage and length. Although the attachment coefficient is larger than the ionization coefficient immediately in front of the cathode, the density of negative ions does not contribute significantly to the space charge until the negative glow. The voltage drop and length of the cathode fall must increase in order to maintain the same net ionization as occurred in a pure electropositive gas.

[1]W. Allis, Revue de Physique Applique'e 10, 97 (1975).
[2]W. Allis, G. Fournier, and D. Pigache, J. de Physique 38, 915 (1977).
[3]J. Boeuf and E. Marode, J. Phys. D 15, 2169 (1982).
[4]J. Boeuf, E. Marode, P. Segur, A. Davies, and J. Evans, Proc. 6th Int. Conf. on Gas Discharges, Edinburgh, IEE Conf. Pub. 189, 2, 63 (1980).
[5]W. Long, Jr., Air Force Aero Propulsion Laboratory Technical Report 79-2038 (1979).
[6]P. Segur, M. Yousfi, and E. Marode, Proc. 6th Int. Conf. on Gas Discharges, Edinburgh, IEE Conf. Pub. 189, 2, 56 (1980).
[7]A. Tran Ngoc, E. Marode, and P. Johnson, J. Phys. D 10, 2317 (1977).
[8]K. Emeleus and J. Sayers, Proc. Royal Irish Acad. 44A, 87 (1938).
[9]L. Christophorou and J. Stockdale, J. Chem. Phys. 48, 1956 (1968).
[10]J. Lucas and H. Saelee, J. Phys. D 8, 640 (1975).
[11]L. Pitchford and A. Phelps, Air Force Wright Aeronautical Laboratory Technical Report 81-2035 (1981).
[12]Y. Sakai, H. Tagashira, and S. Sakamoto, J. Phys. D 10, 1035 (1977).
[13]D. Kreider, R. Kuller, D. Ostberg, and F. Perkins, An Introduction to Linear Analysis (Addison-Wesley, Reading, MA, 1966) Ch 2-9.
[14]A. Ward, J. Appl. Phys. 33, 2789 (1962).
[15]F. Merritt, Mathematics Manual (McGraw-Hill, New York, 1962).
[16]D. Rapp and P. Englander-Golden, J. Chem. Phys. 43, 1464 (1965).
[17]L. Kieffer, "A Compilation of Electron Collision Cross Section Data for Modeling Gas Discharge Lasers", JILA Information Center Report 13 (1973).
[18]M. Hayashi, J. de Physique 40-c7, 45 (1979).
[19]G. Duke, Air Force Wright Aeronautical Laboratories Technical Report 84-2099 (1984).
[20]D. Davies, Air Force Wright Aeronautical Laboratories Technical Report 82-2083 (1983).

END

8-87

DTIC